Geophysical Research Letters

RESEARCH LETTER
10.1029/2018GL079986

The Cold Transit of Southern Ocean Upwelling

Dafydd Gwyn Evans[1], **Jan D. Zika**[2], **Alberto C. Naveira Garabato**[1], **and A. J. George Nurser**[3]

[1]Ocean and Earth Science, National Oceanography Centre Southampton, University of Southampton, Southampton, UK, [2]School of Mathematics and Statistics, University of New South Wales, Sydney, New South Wales, Australia, [3]National Oceanography Centre, Southampton, UK

Key Points:
- Volumetric distribution reveals new thermohaline pathway for transformation of Circumpolar Deep Water to intermediate water
- Transformation pathway relies on seasonal cycle of air-ice-sea buoyancy fluxes
- Upwelling of deep water is sensitive to nonlinearities in the equation of state for sea water

Supporting Information:
- Supporting Information S1
- Movie S1
- Movie S2

Correspondence to:
D. G. Evans,
dafydd.evans@noc.soton.ac.uk

Citation:
Evans, D. G., Zika, J. D., Naveira Garabato, A. C., & Nurser, A. J. G. (2018). The cold transit of Southern Ocean upwelling. *Geophysical Research Letters*, *45*. https://doi.org/10.1029/2018GL079986

Received 9 AUG 2018
Accepted 2 DEC 2018
Accepted article online 5 DEC 2018

Abstract The upwelling of deep waters in the Southern Ocean is a critical component of the climate system. The time and zonal mean dynamics of this circulation describe the upwelling of Circumpolar Deep Water and the downwelling of Antarctic Intermediate Water. The thermodynamic drivers of the circulation and their seasonal cycle play a potentially key regulatory role. Here an observationally constrained ocean model and an observation-based seasonal climatology are analyzed from a thermodynamic perspective, to assess the diabatic processes controlling overturning in the Southern Ocean. This reveals a seasonal two-stage cold transit in the formation of intermediate water from upwelled deep water. First, relatively warm and saline deep water is transformed into colder and fresher near-surface winter water via wintertime mixing. Second, winter water warms to form intermediate water through summertime surface heat fluxes. The mixing-driven pathway from deep water to winter water follows mixing lines in thermohaline coordinates indicative of nonlinear processes.

Plain Language Summary Deep, cold and salty water is drawn to the surface ocean around Antarctica. This is controlled by the combined action of winds blowing over the sea surface and the stirring by large 100-km eddies. Studying the ocean around Antarctica is notoriously challenging. We therefore have sparse ocean measurements in this region. This limits our understanding of some of the processes involved in the circulation of deep water, notably, a stage involving the warming and freshening of deep water to form intermediate water. Intermediate water plays a key role in drawing excess anthropogenic heat and carbon dioxide from the sea surface into the interior ocean. Our results show that the conversion of deep to intermediate water involves a two-stage "cold transit" that takes place over the course of the austral season. First, during the winter, deep water sits below the very cold and fresh surface water. Ice formation around Antarctica makes this surface water slightly saltier, decreasing the density difference between the deep and surface water. This drives a mixing which cools and freshens the deep water while drawing it to the surface. Second, during summer surface warming and melting sea ice warm and freshen this deep/surface water mixture forming intermediate water.

1. Introduction

The upwelling, transformation, and downwelling of water masses in the Southern Ocean exerts a profound influence on the heat, freshwater, and carbon budgets of the world ocean (Iudicone et al., 2011; Purkey & Johnson, 2010; Rintoul & Naveira-Garabato, 2013; Sabine et al., 2004; Talley, 2013). This residual meridional overturning circulation (MOC; Marshall & Speer, 2012) is thought to be governed by a balance between wind-driven upwelling/downwelling, eddy-induced advection and stirring, diapycnal mixing, and air-ice-sea buoyancy fluxes (Abernathey et al., 2011; Naveira Garabato et al., 2007; Speer et al., 2000; Zika et al., 2009). The prevailing westerly winds over the Southern Ocean drive an equatorward mass transport near the surface, causing upwelling poleward and downwelling equatorward of the zonal wind stress maximum. From a dynamical point of view, this tilts isopycnals and sets up the geostrophic eastward flow of the Antarctic Circumpolar Current. Baroclinic instabilities within the Antarctic Circumpolar Current generate eddies that act to shoal isopycnals, balancing the action of the winds (Marshall & Radko, 2003). From a water mass point of view, transient and stationary eddies compensate for the wind-driven circulation by pushing dense waters downward and northward and lifting light waters upward and poleward. Ultimately, the only water that flows northward is that which is diabatically transformed from dense water by air-sea buoyancy fluxes and diapycnal mixing (Pellichero et al., 2018; Speer et al., 2000).

©2018. American Geophysical Union. All Rights Reserved.

The diabatic processes that convert dense waters to lighter waters, and the seasonal cycle in that conversion, are poorly understood. This not only hinders accurate estimates of the Southern Ocean MOC but also limits our ability to predict its fate in a changing climate (Downes et al., 2009; Fyfe & Saenko, 2006; Morrison et al., 2015; Thomas et al., 2015). Most conceptual views of the Southern Ocean MOC use time mean values for air-ice-sea buoyancy fluxes to explain the net transformation of Upper and Lower Circumpolar Deep Water (hereinafter "deep water") into either Antarctic Bottom Water (hereinafter "bottom water") or Antarctic Intermediate Water (hereinafter "intermediate water"; Cerovečki et al., 2013; Czaja & Marshall, 2015, Karsten & Marshall, 2002).

Intermediate water formation and subduction form the downwelling limb of the Southern Ocean MOC's upper cell (Speer et al., 2000). A net warming and freshening of upwelled deep water into the less dense intermediate water typically occurs in the vicinity of the Polar Front (Pellichero et al., 2018). This transformation is predominantly driven by a net freshening associated with sea ice export and melt (Abernathey et al., 2016; Pellichero et al., 2018). Further, a recent analysis of Lagrangian upwelling pathways in the Southern Ocean indicates that this upwelling deep water may initially become colder and fresher upon reaching the surface mixed layer before forming intermediate water (Tamsitt et al., 2018). This hints at the importance of considering seasonally varying air-ice-sea buoyancy fluxes in setting the strength of the Southern Ocean MOC (Evans et al., 2014).

Using both models and observations, we investigate the seasonal variation in the transformations of water masses in the Southern Ocean, to assess the role of air-ice-sea fluxes and diapycnal mixing in setting the seasonal formation and destruction of deep water, intermediate water, and Antarctic winter water (hereinafter "winter water") which forms the winter mixed layer south of the Polar Front. We show that the seasonal evolution of the air-ice-sea buoyancy fluxes plays a critical role in the wintertime upwelling of deep water through mixing with overlying winter water. Summertime warming and freshening forms intermediate water through heat exchange with the atmosphere and sea ice melt. Close inspection of the mixing-driven pathway from deep water to winter water in thermohaline coordinates suggests a strong association with nonlinear mixing processes.

In the ocean, nonlinear mixing processes are represented by nonlinear terms in the equation of state (EOS) of seawater (McDougall, 1987). This nonlinear dependence of density on temperature and salinity leads to curious effects such as cabbeling, where two water parcels can be mixed to form water that is denser than either parcel. Thermobaricity is another nonlinear processes that relates to the effect of pressure on the thermal expansion of water, whereby large pressure changes induce larger density changes in colder water. Such nonlinear effects are generally thought to be obscure despite early studies that indicated their importance for the overturning circulation in the ocean (Fofonoff, 1957; Foster & Carmack, 1976). Fofonoff (1957), for example, analyzed profiles of temperature and salinity in the Weddell Sea and suggested that cabbeling was a rate-limiting process in the formation of bottom water and the lower limb of the Southern Ocean MOC. Recent studies have since highlighted the importance of EOS nonlinearities in setting the formation of intermediate water (Groeskamp et al., 2016; Nycander et al., 2015). Here we suggest that cabbeling may indeed be of critical importance to the strength of the Southern Ocean overturning but in relation to the upwelling and transformation of deep waters into intermediate waters.

2. Methodology

The aim of this analysis is to understand the role of temperature (Θ) and salinity (S) transformations in Southern Ocean overturning. Walin (1982) introduced a framework to relate the intensity of surface heat fluxes and mixing to transformation rates. He compared volumes of water in Θ classes to the diasurface transformations of water between Θ classes affected by air-sea heat fluxes and mixing. Here we extend this analysis to two tracer dimensions, Θ and S (Döös et al., 2012; Groeskamp et al., 2014; Zika et al., 2012), and to a time-varying ocean (Evans et al., 2014).

Consider the total volume of water per unit temperature and salinity for a particular geographical region (V; Worthington, 1981). Since seawater is, to a good approximation, incompressible, V can only increase or decrease in this region if water enters from the boundaries via horizontal advection or air-sea exchange (M, the volume transport per unit temperature and salinity) or through transformation of water within the region across isotherms (G_Θ, the transformation across an isotherm per unit salinity) or across isohalines (G_S, the

transformation across an isohaline per unit temperature) such that

$$\frac{dV}{dt} = M - \frac{\partial G_\Theta}{\partial \Theta} - \frac{\partial G_S}{\partial S}. \quad (1)$$

Above, the G terms can be thought of as analogous to velocity in (Θ, S) coordinates, and so (1) can be seen as a continuity equation in (Θ, S) space. If a sufficiently long time integration is considered such that the system is steady (i.e., $\overline{dV/dt} = 0$, where the overbar is a time mean) and if $\overline{M}$ is small (i.e., for the global ocean or when water masses below particular Θ and S values are never in contact with the boundaries) a thermohaline streamfunction (Ψ; Döös et al., 2012; Groeskamp et al., 2014; Zika et al., 2012) can be defined at $\Theta = \Theta^*$ and $S = S^*$ such that

$$\Psi(\Theta^*, S^*) = -\int_{\min(S)}^{S^*} \overline{G_\Theta(\Theta^*, S)} dS \approx \int_{\min(\Theta)}^{\Theta^*} \overline{G_S(\Theta, S^*)} d\Theta. \quad (2)$$

As discussed by Hieronymus et al. (2014), both transformation terms (G_Θ and G_S), and hence the streamfunction, can be related purely to diabatic convergences of heat and salt. Following this, Evans et al. (2014) and Groeskamp et al. (2017) were able to use the seasonal cycle of V and observation-based estimates of air-sea fluxes to estimate both G terms via an inverse calculation.

Here we focus on understanding the mean circulation of Southern Ocean water masses in (Θ, S) coordinates (Ψ), and how this circulation emerges from the seasonal cycle of water mass formation and destruction described by (1).

3. Data Sources

To determine V, we use an observation-based seasonal climatology and an ocean state estimate. The seasonal climatology we use is the CSIRO (Commonwealth Scientific and Industrial Research Organisation) Atlas of Regional Seas (CARS) 2009 (Ridgway et al., 2002), accessed at www.cmar.csiro.au/cars. CARS is a global atlas of seasonal water mass properties with a horizontal resolution of 1/2° that extends to 75°S, derived from all available subsurface data. Using CARS, year-round seasonal-mean estimates of Conservative Temperature and Absolute Salinity (IOC et al., 2010) are calculated from a mean field and the semiannual and annual components of the seasonal cycle, extending from the surface to 1,000 m.

The state estimate used here is the Estimating the Circulation and Climate of the Ocean version 4 (ECCOv4; Forget & Ponte, 2015). ECCOv4 uses an adjoint model to find the best fit between the state estimate and any available observational data by adjusting the initial conditions of the model. Here we use monthly fields (1992–2012) for potential temperature, practical salinity, air-sea and ice-sea fluxes, and 3-D velocity (including parameterized subgrid eddy advection). We use ECCOv4 to compute V and the transformation rates due to air-ice-sea fluxes and mixing that combine to give G in equation (2). These data are accessed via https://ecco.jpl.nasa.gov/. Both Conservative Temperature (CARS) and potential temperature (ECCOv4) will be referred to by Θ, while Absolute Salinity (CARS) will be referred to by S_A and practical salinity (ECCOv4) by S. To calculate density from Conservative Temperature and Absolute Salinity, we use TEOS-10, while we use EOS-80 for density calculations involving potential temperature and practical salinity. Although ECCOv4 and CARS use some of the same observational data in producing the final output of each product, the implementation of these observational data is very different. Any features that are consistent between ECCOv4 and CARS are more likely to be independent of the methods specific to each product.

Transformation rates in ECCOv4 are computed using both the velocity down the tracer gradient and the rate of movement of the tracer isosurface (Groeskamp et al., 2014). The 3-D velocity includes contributions from both the Eulerian velocity and the eddy velocity, which results from parameterized subgrid scale physics. It is the sum of these velocities that advects Θ and S. The contribution of air-sea and ice-sea fluxes to these transformations is computed following Evans et al. (2014). We do not account for the effects of shortwave radiation depth penetration, which has little effect on the derived transformations in the Southern Ocean (Groeskamp & Iudicone, 2018). The mixing component is inferred as the residual of the total transformation and air-ice-sea flux-driven transformation. Hence, this includes potential contributions from both explicit mixing and implicit mixing linked to discretization and the advection scheme of the ocean model underpinning ECCOv4 (MITgcm).

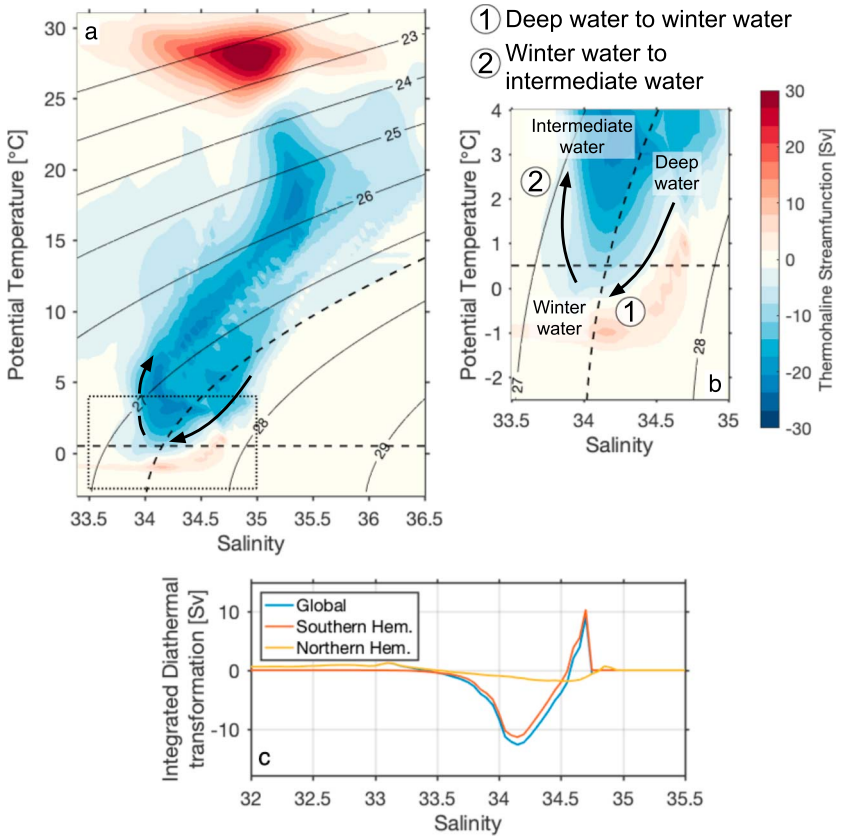

Figure 1. (a) Global estimate of the thermohaline streamfunction (Ψ) from ECCOv4. Black contours show density anomaly referenced to 0 dbar (σ_0). The dashed box highlights the area shown in panel (b). In both (a) and (b), the dashed black lines showing the isotherm at 0.5 °C and the isopycnal at σ_0 = 27.4 kg/m^3 approximately separate the water masses considered here: deep water ($\Theta > 0.5$°C, $\sigma_0 > 27.4$ kg/m^3), winter water ($\Theta < 0.5$°C) and intermediate water ($\Theta > 0.5$°C, $\sigma_0 < 27.4$ kg/m^3). (c) Transformation rate across the 0.5 °C isotherm for the global ocean and for each of the Northern and Southern Hemispheres.

4. A Southern Ocean "Cold Transit" of the Thermohaline Circulation

In this section, we describe the global thermohaline streamfunction and its variability in ECCOv4 and demonstrate the dominance of Southern Ocean processes in the cold and fresh corner of the (Θ, S) diagram. The global estimate of Ψ from ECCOv4 confirms the existence of two minor anticlockwise cells, one at the warmest temperatures and another at the coldest temperatures (red contours; Figure 1a), and of one major clockwise cell spanning the majority of the temperatures observed in the world ocean (blue contours; Figure 1a).

In the clockwise cell, approximately 20 Sv (1 Sv = 10^6m^3/s) of water undergo the following sequence of transformations: (a) relatively cool and fresh water is warmed; (b) warm, fresh water is salinified; (c) warm, saline water is cooled to form dense water (the densest waters are in the cold-saline corner of the diagram, with the dashed contour showing the 27.4 kg/m^3 isopycnal); and (d) cold, saline water is freshened. Zika et al. (2012) and Döös et al. (2012) found that this cell was consistent with descriptions of the "global conveyor" or global thermohaline circulation, with densification and sinking occurring in the North Atlantic, upwelling and freshening occurring in the Southern Ocean, and warming and salinification along broad return routes via the surface of all the world's ocean basins.

These data enable us to corroborate the dominance of the Southern Ocean in the freshening route within an observationally constrained model and to assess the processes underpinning these transformations. Of interest here are the coldest and freshest water masses in the world ocean and the Southern Ocean's role in their modification. Figure 1b shows Ψ in the area of thermohaline space occupied by these water masses, with three distinct water types highlighted: deep water ($\Theta > 0.5$°C and $\sigma_0 > 27.4$ kg/m^3); winter water ($\Theta \leq 0.5$°C); and intermediate water ($\Theta > 0.5$°C, $\Theta < 3$°C, and $\sigma_0 < 27.4$ kg/m^3). This shows that deep water is converted

to intermediate water through winter water. The freshening branch involves an approximate ratio of 0.4 g/kg of freshening for every 2 °C of cooling. The warming branch involves very little freshening.

To provide a simple quantification of the Southern Ocean's prevalence in shaping Ψ at low temperatures, we compare contributions to the transformation rate across the 0.5 °C isotherm ($\Psi|_{\Theta=0.5°C}$) from the Southern and Northern Hemispheres separately (Figure 1c). We find that 12.7 Sv crosses the 0.5°C isotherm from cold to warm temperatures at waters fresher than 34.1 g/kg (arrow 2 in Figure 1b). Later we show that this transformation is set by air-ice-sea buoyancy fluxes. Of this transformation, 11.4 Sv (~ 90%) occurs in the Southern Hemisphere. At higher salinities, approximately 21 Sv crosses the 0.5°C isotherm from warm to cold temperatures (arrow 1 in Figure 1b). As discussed in section 5 this transformation is set by subsurface mixing. This is the sum of a 26 Sv transformation from warm to cold in the Southern Hemisphere, balanced by 10 Sv from cold to warm elsewhere. Computing a Southern Hemisphere-only streamfunction for cold, fresh waters, confirms the dominance of Southern Hemisphere processes in this part of the global thermohaline circulation (Figure S1 and the supporting information). In summary, ECCOv4 shows a prominence of a cold transit (below 0.5 °C) in the global thermohaline circulation. Via this cold transit, saline deep water is transformed into fresh intermediate water, through the cold and fresh winter water. These transformations take place almost exclusively in the Southern Ocean.

5. Seasonal Cycle of Water Mass Transformations

Having shown that the transformation of saline deep water into fresh intermediate water occurs via a Southern Ocean cold transit of the thermohaline circulation, in this section we demonstrate that this cold transit is linked to the seasonal cycle of air-ice-sea buoyancy fluxes and subsurface mixing. Pronounced seasonality occurs in the bulk volumes of winter water, intermediate water, and deep water, in both CARS (Figure 2b) and ECCOv4 (Figure 2a). Winter water experiences the largest variation, with maximum volume toward the end of the austral winter in October, and minimum volume during the summer in March. Intermediate water volume reaches a maximum during the summer in February and a minimum in August. Deep water volume is highest during June and July and attains a minimum in October—suggesting a relatively rapid depletion of deep water between July and October (4 months), with a gradual recharge between October and June (8 months).

These bulk volume changes can be related to seasonal variations in the distribution of water in (Θ, S) space (Figures 2c–2f; here we show ECCOv4 only, but CARS exhibits very similar structures: see Figure S2). The volumetric distribution in (Θ, S) space forms a dominant ridge of high volume that begins with intermediate water (I; Figure 2), at the warmest and freshest Θ and S shown in Figures 2c–2f. This ridge then bends toward the higher salinities characteristic of deep water (II; Figure 2) and finally back toward the lower Θ and S associated with bottom water (III; Figure 2). Also evident are two minor ridges of elevated volume that connect winter water to deep water, and winter water to intermediate water (marked by red lines in Figure 2c). During the transition from summer (December; Figures 2d and 2f) to winter (August; Figures 2c and 2e), there is a redistribution of volume between intermediate water and winter water, indicative of cooling and the formation of the winter mixed layer. The coldest of this water further shifts to a higher salinity, close to that of the ridge connecting winter water to deep water, through brine rejection linked to sea ice formation. During the transition from winter to summer, warming and freshening redistributes volume from winter water into intermediate water. The seasonal variations of water mass volume in (Θ, S) space are also shown in Movie S1 and Figure S3.

The respective roles of air-ice-sea buoyancy fluxes and subsurface mixing in the transformation of water between different (Θ, S) classes can be understood by comparing the vector fields of the diasurface transformation due to air-ice-sea buoyancy fluxes and the diasurface transformation due to subsurface mixing (Evans et al., 2014, 2017). Wintertime surface cooling drives the negative diathermal transformation converting intermediate water into winter water (Figure 2c). Near $\Theta = -1.8$ °C and at $S > 34$, a positive diahaline transformation driven by sea ice formation and brine rejection forms a salty type of winter water, with a maximum S of ~34.4. In addition, subsurface mixing induces a negative transformation across isotherms and isohalines that brings about a cooling and freshening of the water along the ridge of high volume connecting winter water to deep water (Figure 2e). This corresponds to arrow 1 in Figure 1, the transformation of deep water to winter water. This mixing between winter water and the underlying deep water coincides with the seasonal reduction in the bulk volume anomaly of deep water (Figures 2a and 2b) and occurs when the newly formed winter water reaches a sufficiently high salinity and density to spur mixing between winter and deep water. The magnitude of the wintertime mixing-driven transformation from deep water to winter

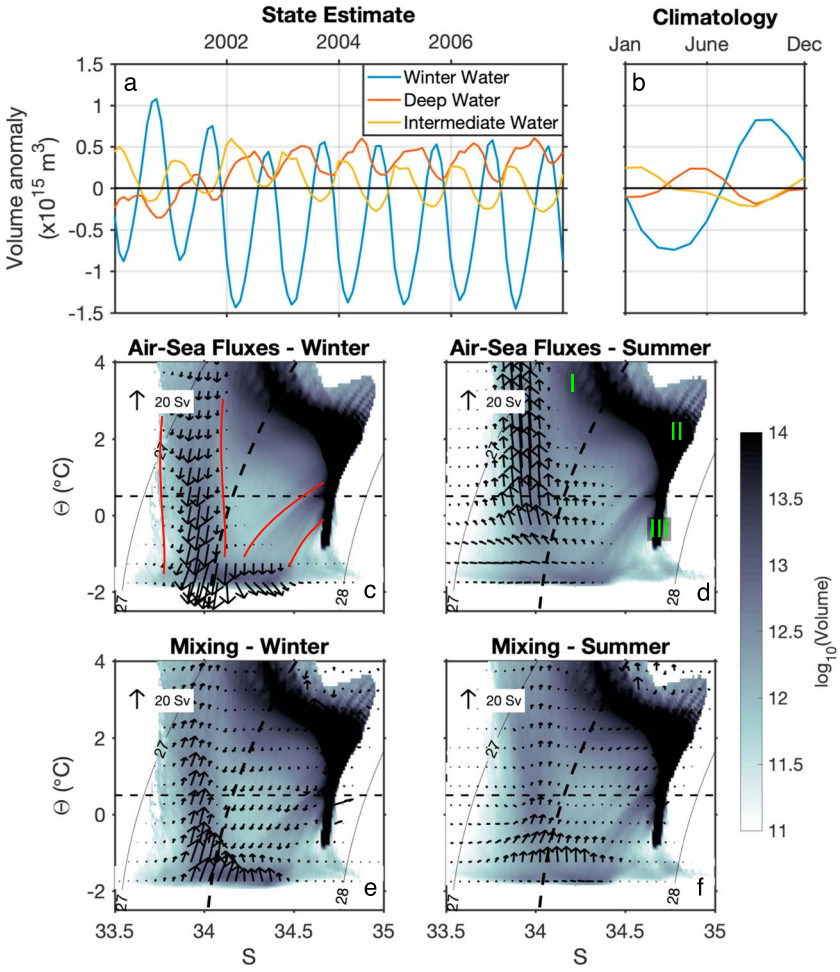

Figure 2. Time series of volume anomaly in (a) ECCOv4 and (b) CARS, for winter water (blue), intermediate water (yellow), and deep water (orange). (c, d) Monthly mean (1992–2012) of $\log_{10}$ volume in (Θ, S) classes (in $m^3/°C/(g/kg)$) for August and December, respectively, from ECCOv4 in the Southern Hemisphere. Black contours show density anomaly referenced to 0 dbar (σ_0), and the thick dashed contour indicates $\sigma_0 = 27.4$ kg/m^3. Black arrows represent vectors of the diasurface transformation due to air-ice-sea buoyancy fluxes averaged over June/July and November, respectively (units: Sv/°C/psu). (e, f) As in (c, d), but black arrows represent vectors of the diasurface transformation due to mixing inferred from the residual volume change in ECCOv4. The red lines indicate the regions of elevated volume connecting deep water to winter water and intermediate water to winter water. I = intermediate water, II = deep water, III = bottom water.

water is equivalent to the total transformation responsible for the formation of the winter mixed layer from surface water masses. Winter water is transformed into intermediate water during spring and summer, as a result of atmospheric warming (a positive diathermal transformation) and freshening linked to sea ice melting (a negative diahaline transformation; Figure 2d). These process are also shown in Movie S1.

The geographical location of this water mass transformation is shown by displaying the location of mixed layer (Θ, S) classes in ECCOv4 (Figure S4 and Movie S2). The wintertime mixing-driven transformations between winter water and deep water typically occur in the Weddell Sea and in the Atlantic sector of the Southern Ocean. This is evident in the warming and salinification of the mixed layer during the winter, which is typically shallower than 200 m (Pellichero et al., 2017).

Our analysis of the seasonal cycle of water mass transformations is shown schematically in Figure 3 and can be summarized as follows: (i) in the autumn and winter, intermediate water is cooled toward the freezing point to form winter water, which is then salinified by brine rejection; (ii) during winter, deep water is transformed into winter water by mixing with the coldest winter water; and (iii) in the spring and summer, winter water is warmed to form intermediate water. In terms of the mean circulation in (Θ, S) coordinates described in the previous section, we can now conclude that the circulation's cooling and freshening branch (arrow 1, Figure 1)

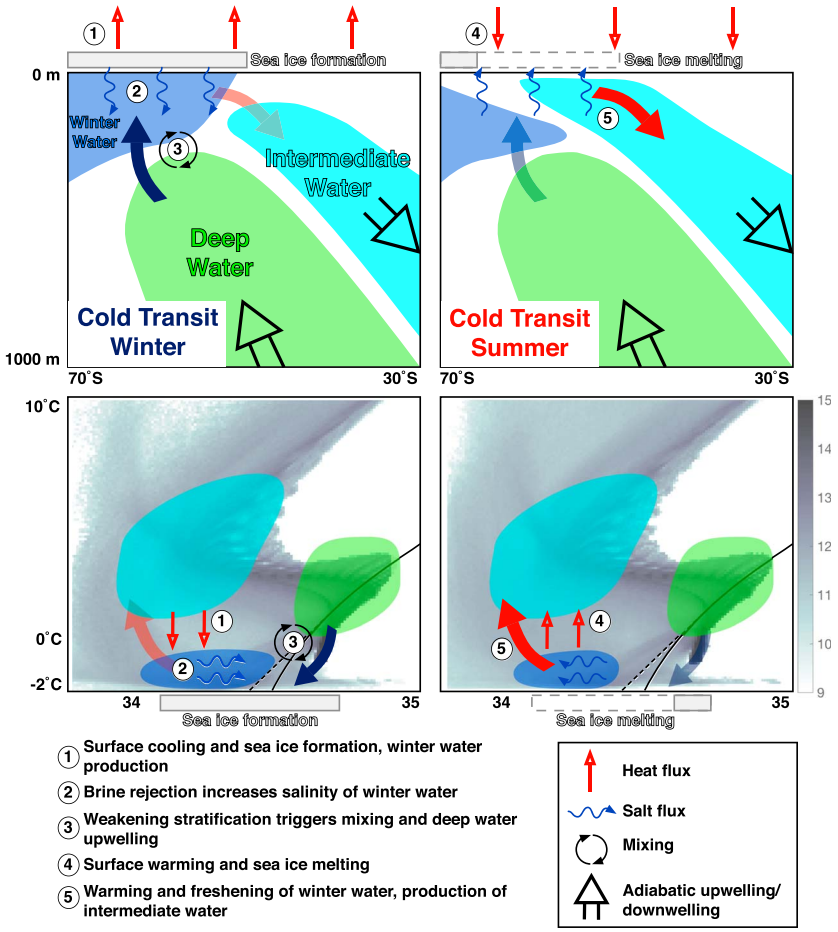

Figure 3. Schematic representation of the diabatic conversion of deep water into intermediate water through winter water, over the course of a season in the Southern Ocean. Each water mass is represented by the colored blobs. The top row presents the changes in geographical coordinates, and the bottom shows the same changes in temperature and salinity coordinates. The large opaque arrows show the water mass transformations that occur during the respective seasons.

is underpinned by wintertime mixing (ii) and that the warming/freshening branch (arrow 2 in Figure 1) is the residual of wintertime atmospheric cooling (i) and summertime warming (iii).

These results are consistent with existing analyses of Southern Ocean water masses. For example, the cooling and freshening of deep water during the wintertime portion of the cold transit is supported by an analysis of the Lagrangian upwelling pathways of deep water by Tamsitt et al. (2018). Further, consistent with the summertime portion of the cold transit, Abernathey et al. (2016), Groeskamp et al. (2016), and Pellichero et al. (2018) describe the role of sea ice melt and the resultant freshwater fluxes in the formation of intermediate water during the summer. However, through their use of a 1-D isopycnal framework rather than the 2-D (Θ, S) framework adopted here, these analyses mask the more subtle seasonal water mass transformations between (Θ, S) classes that we highlight. Our results therefore provide a clearer definition of the diabatic processes that link the upwelling and downwelling limbs of the Southern Ocean overturning.

6. The Role of Nonlinear Mixing Processes in the Southern Ocean Cold Transit

Subsurface mixing drives a wintertime transformation of relatively warm and saline deep water into cold and fresh winter water. Close inspection of the volumetric water mass distribution (Figures 2c–2f) reveals that the ridges of water mass volume (red lines Figure 2c) extend from the deep water to the dominant mode of near-freezing winter water (between 34.3 and 34.4 g/kg, and −1.8 and −1.5 °C). Examining the mixing-driven transformation vectors in ECCOv4, we find that the wintertime mixing-driven cooling of deep water to winter water is aligned with these ridges.

An important aspect of this pathway from deep water to winter water (arrow 1 in Figure 1b) is that the ridge in the volumetric distribution and the transformation vectors are not as "steep" as density contours. This implies that the dense water becomes lighter (rather than denser) upon mixing. It therefore discourages suggestions that the deep water is transformed into winter water through gravitational instability or convection. This would imply a densification of both winter water and deep water. Although we cannot definitively rule out a mechanical driver (such as breaking internal waves, shear instabilities or entrainment into the mixed layer via wind and wave driven turbulence), we suggest that this transformation may be consistent with a mixing mechanism related to nonlinearities in the EOS of seawater.

Although they are typically considered obscure, recent work has shown that EOS nonlinearities have important consequences for global ocean circulation and climate. Nycander et al. (2015) and Groeskamp et al. (2016) show that the isopycnal mixing of cold/fresh surface water with deeper warmer/saltier water results in a cabbeling-induced densification that forms intermediate water density classes. In addition to its role in the lateral mixing of waters with the same locally referenced potential density, the role of cabbeling in vertical stability has also been long recognized. Fofonoff (1957) and Foster (1972) speculated that, for example, cabbeling may play a role in bottom water formation. They point out that a small amount of mechanically driven wintertime mixing between cold/fresh winter water and warm/salty deep water can produce a mixture that is denser than the deeper of the two water masses, initiating a cabbeling instability that drives enhanced mixing between winter water and deep water. Foster and Carmack (1976) further suggest that thermobaricity has a minimal impact on the mixing between deep water and winter water. Su et al. (2016) also highlight the role of EOS nonlinearities in driving vertical mixing when cold/fresh water overlies warm/salty water, emphasizing in particular the importance of cabbeling. Here we conjecture that the nonlinear mixing that upwells deep water via the cold transit may also be a consequence of cabbeling. The nonlinear mixing occurs when cold/fresh winter water overlies warm/salty deep water, through a depth range spanning less that 200 m. It is possible therefore that this mixing is the result of a similar cabbeling instability to that described by Foster (1972) and Foster and Carmack (1976).

7. Summary and Conclusions

Conventional theory of Southern Ocean overturning is based on the balance between the competing actions of winds, which tilt isopycnal surfaces, and mesoscale eddies, which flatten isopycnal surfaces. The resulting residual overturning circulation entails upwelling of deep water south of the Polar Front and downwelling of intermediate water and overlying Subantarctic Mode Water north of the Polar Front (Marshall & Radko, 2003). The diabatic conversion of deep water into intermediate water (or bottom water near the Antarctic margins) is thought to depend on the location in which deep water upwells into the upper-ocean mixed layer, relative to the local sign of the time mean air-ice-sea buoyancy flux (Marshall & Speer, 2012; Speer et al., 2000). However, recent studies highlight the role of seasonally varying air-ice-sea buoyancy fluxes in intermediate water formation (Abernathey et al., 2016; Groeskamp et al., 2016; Pellichero et al., 2018).

By projecting the Southern Ocean into (Θ, S) space, we have shown that the diabatic conversion of deep water into intermediate water relies on seasonal variations of surface buoyancy forcing and subsurface mixing. This presents an alternative pathway for the diabatic conversion of deep water via a cold transit in (Θ, S) space, in which deep water is first cooled and freshened during the winter, as it mixes with overlying winter water. Summertime warming and freshening of this winter water/deep water mixture subsequently forms intermediate water. These diabatic transformations occur predominantly in the Weddell Sea and the Atlantic sector of the Southern Ocean. An analysis of the Lagrangian upwelling pathways of deep water by Tamsitt et al. (2018) supports the notion that deep water becomes cooler and fresher as it is entrained into the winter mixed layer. In our analysis, the use of a (Θ, S) framework in combination with air-ice-sea buoyancy flux data reveals important seasonal variations that would otherwise be lost using an isopycnal framework, where the variability of water masses with similar densities but a differing (Θ, S) would be collapsed into one density class. The cold transit may therefore be masked by the use of isopycnal frameworks in previous analyses of these water masses.

The transformation of dense deep water into lighter upper-ocean mixed layer water by subsurface mixing apparently occurs when the salinity of winter water is increased as brine is rejected by newly forming sea ice. We propose that this critical salinity occurs when the overlying winter water and underlying deep water can

be mixed to form a water mass that is denser than the deep water or more specifically when the water column is unstable to cabbeling.

In conclusion, an increasing body of evidence suggests that seasonal variations in air-ice-sea buoyancy fluxes and their impact on subsurface mixing play a key role in the diabatic closure of the MOC in the Southern Ocean. Our analysis indicates that the transformation of deep waters into intermediate waters occurs via a transit through cold winter water and that this cold transit is mediated by nonlinear mixing processes. These findings advance our ability to estimate the drivers of Southern Ocean overturning and therefore its response to forcing changes in past and future climates.

Acknowledgments

D. G. E. was supported by a Natural Environment Research Council studentship award at the University of Southampton. J. D. Z. was supported by the Australian Research Council (grant DP160103130). A. C. N. G. gratefully acknowledges support from the Leverhulme Trust, the Royal Society, and the Wolfson Foundation. The contribution of A. J. G. N. was supported by the NERC grant Ocean Regulation of Climate by Heat and Carbon Sequestration and Transports (ORCHESTRA) (NE/N018095/1). ECCO data are available for download here: https://ecco.jpl.nasa.gov/. CARS data are available for download here: http://www.marine.csiro.au/~dunn/cars2009/. We also thank Sjoerd Groeskamp and an anonymous reviewer for their helpful and constructive comments on this manuscript.

References

Abernathey, R. P., Cerovecki, I., Holland, P. R., Newsom, E., Mazloff, M., & Talley, L. D. (2016). Water-mass transformation by sea ice in the upper branch of the Southern Ocean overturning. *Nature Geoscience*, *9*, 596–601.

Abernathey, R., Marshall, J., & Ferreira, D. (2011). The dependence of Southern Ocean meridional overturning on wind stress. *Journal of Physical Oceanography*, *41*(12), 2261–2278. https://doi.org/10.1175/JPO-D-11-023.1

Cerovečki, I., Talley, L. D., Mazloff, M. R., & Maze, G. (2013). Subantarctic mode water formation, destruction, and export in the eddy-permitting Southern Ocean state estimate. *Journal of Physical Oceanography*, *43*(7), 1485–1511. https://doi.org/10.1175/JPO-D-12-0121.1

Czaja, A., & Marshall, J. (2015). Why is there net surface heating over the Antarctic Circumpolar Current? *Ocean Dynamics*, *65*(5), 751–760. https://doi.org/10.1007/s10236-015-0830-1

Döös, K., Nilsson, J., Nycander, J., Brodeau, L., & Ballarotta, M. (2012). The World Ocean thermohaline circulation. *Journal of Physical Oceanography*, *42*(9), 1445–1460. https://doi.org/10.1175/JPO-D-11-0163.1

Downes, S. M., Bindoff, N. L., & Rintoul, S. R. (2009). Impacts of climate change on the subduction of mode and intermediate water masses in the Southern Ocean. *Journal of Climate*, *23*, 6526–6541. https://doi.org/https://doi.org/10.1175/2010JCLI3620.1

Evans, D. G., Toole, J., Forget, G., Zika, J. D., Naveira Garabato, A. C., Nurser, A. J. G., & Yu, L. (2017). Recent wind-driven variability in Atlantic water mass distribution and meridional overturning circulation. *Journal of Physical Oceanography*, *47*(3), 633–647. https://doi.org/10.1175/JPO-D-16-0089.1

Evans, D. G., Zika, J. D., Naveira Garabato, A. C., & Nurser, A. J. G. (2014). The imprint of Southern Ocean overturning on seasonal water mass variability in Drake Passage. *Journal of Geophysical Research: Oceans*, *119*, 7987–8010. https://doi.org/10.1002/2014JC010097

Fofonoff, N. P. (1957). Some properties of sea water influencing the formation of Antarctic Bottom Water. *Deep Sea Research (1953)*, *4*, 32–35. https://doi.org/https://doi.org/10.1016/0146-6313(56)90029-6

Forget, G., & Ponte, R. M. (2015). The partition of regional sea level variability. *Progress in Oceanography*, *137*, 173–195. https://doi.org/10.1016/j.pocean.2015.06.002

Foster, T. D. (1972). An analysis of the cabbeling instability in sea water. *Journal of Physical Oceanography*, *2*(3), 294–301. https://doi.org/10.1175/1520-0485(1972)002<0294:AAOTCI>2.0.CO;2

Foster, T. D., & Carmack, E. C. (1976). Temperature and salinity structure in the Weddell Sea. *Journal of Physical Oceanography*, *6*(1), 36–44. https://doi.org/10.1175/1520-0485(1976)006<0036:TASSIT>2.0.CO;2

Fyfe, J. C., & Saenko, O. A. (2006). Simulated changes in the extratropical Southern Hemisphere winds and currents. *Geophysical Research Letters*, *33*, L06701. https://doi.org/10.1029/2005GL025332

Groeskamp, S., Abernathey, R. P., & Klocker, A. (2016). Water mass transformation by cabbeling and thermobaricity. *Geophysical Research Letters*, *43*, 10,810–835,845. https://doi.org/10.1002/2016GL070860

Groeskamp, S., & Iudicone, D. (2018). The effect of air-sea flux products, shortwave radiation depth penetration, and albedo on the upper ocean overturning circulation. *Geophysical Research Letters*, *45*, 9087–9097. https://doi.org/10.1029/2018GL078442

Groeskamp, S., Sloyan, B. M., Zika, J. D., & McDougall, T. J. (2017). Mixing inferred from an ocean climatology and surface fluxes. *Journal of Physical Oceanography*, *47*(3), 667–687. https://doi.org/10.1175/JPO-D-16-0125.1

Groeskamp, S. J., Zika, J. D., McDougall, T. J., Sloyan, B. M., & Laliberté, F. (2014). The representation of ocean circulation and variability in thermodynamic coordinates. *Journal of Physical Oceanography*, *44*, 1735–1750. https://doi.org/10.1175/JPO-D-13-0213.1

Hieronymus, M., Nilsson, J., & Nycander, J. (2014). Water mass transformation in salinity–temperature space. *Journal of Physical Oceanography*, *44*(9), 2547–2568. https://doi.org/10.1175/JPO-D-13-0257.1

IOC, SCOR, & IAPSO (2010). The international thermodynamic equation of seawater—2010: Calculation and use of thermodynamic properties. Intergovernmental Oceanographic Commission, manuals an ed.

Iudicone, D., Rodgers, K. B., Stendardo, I., Aumont, O., Madec, G., Bopp, L., et al. (2011). Water masses as a unifying framework for understanding the Southern Ocean carbon cycle. *Biogeosciences*, *8*(5), 1031–1052. https://doi.org/10.5194/bg-8-1031-2011

Karsten, R. H., & Marshall, J. (2002). Constructing the residual circulation of the ACC from observations. *Journal of Physical Oceanography*, *32*, 3315–3327.

Marshall, J., & Radko, T. (2003). Residual-mean solutions for the Antarctic Circumpolar Current and its associated overturning circulation. *Journal of Physical Oceanography*, *33*(11), 2341–2354. https://doi.org/10.1175/1520-0485(2003)033<2341:RSFTAC>2.0.CO;2

Marshall, J., & Speer, K. (2012). Closure of the meridional overturning circulation through Southern Ocean upwelling. *Nature Geoscience*, *5*(3), 171–180.

McDougall, T. J. (1987). Thermobaricity, cabbeling, and water–mass conservation. *Journal of Geophysical Research*, *92*(C5), 5448–5464.

Morrison, A. K., England, M. H., & Hogg, A. M. (2015). Response of Southern Ocean convection and abyssal overturning to surface buoyancy perturbations. *Journal of Climate*, *28*(10), 4263–4278. https://doi.org/10.1175/JCLI-D-14-00110.1

Naveira Garabato, A. C., Stevens, D. P., Watson, A. J., & Roether, W. (2007). Short-circuiting of the overturning circulation in the Antarctic Circumpolar Current. *Nature*, *447*, 194–197. https://doi.org/10.1038/nature05832

Nycander, J., Hieronymus, M., & Roquet, F. (2015). The nonlinear equation of state of sea water and the global water mass distribution. *Geophysical Research Letters*, *42*, 7714–7721. https://doi.org/10.1002/2015GL065525

Pellichero, V., Sallée, J.-B., Chapman, C. C., & Downes, S. M. (2018). The Southern Ocean meridional overturning in the sea-ice sector is driven by freshwater fluxes. *Nature Communications*, *9*(1), 1789. https://doi.org/10.1038/s41467-018-04101-2

Pellichero, V., Sallée, J.-B., Schmidtko, S., Roquet, F., & Charrassin, J.-B. (2017). The ocean mixed layer under Southern Ocean sea-ice: Seasonal cycle and forcing. *Journal of Geophysical Research: Oceans*, *122*, 1608–1633. https://doi.org/10.1002/2016JC011970

Purkey, S. G., & Johnson, G. C. (2010). Warming of global abyssal and deep Southern Ocean waters between the 1990s and 2000s: Contributions to global heat and sea level rise budgets*. *Journal of Climate*, *23*(23), 6336–6351. https://doi.org/10.1175/2010JCLI3682.1

Ridgway, K. R., Dunn, J. R., & Wilkin, J. L. (2002). Ocean interpolation by four-dimensional weighted least squares—Application to the waters around Australasia. *Journal of Atmospheric and Oceanic Technology*, *19*(9), 1357–1375. https://doi.org/10.1175/1520-0426(2002)019<1357:OIBFDW>2.0.CO;2

Rintoul, S. R., & Naveira-Garabato, A. C. (2013). Dynamics of the Southern Ocean circulation. In G. Siedler, et al. (Eds.), *Ocean circulation and climate, 2nd Edition: A 21st century perspective* (pp. 471–492). Oxford GB: Academic Press.

Sabine, C. L., Feely, R. A., Gruber, N., Key, R. M., Lee, K., Bullister, J. L., et al. (2004). The oceanic sink for anthropogenic CO_2. *Science*, *305*, 367–371.

Speer, K. G., Rintoul, S. R., & Sloyan, B. M. (2000). The diabatic Deacon cell. *Journal of Physical Oceanography*, *30*, 3212–3222.

Su, Z., Ingersoll, A. P., Stewart, A. L., & Thompson, A. F. (2016). Ocean convective available potential energy. Part II: Energetics of thermobaric convection and thermobaric cabbeling. *Journal of Physical Oceanography*, *46*(4), 1097–1115. https://doi.org/10.1175/JPO-D-14-0156.1

Talley, L. D. (2013). Closure of the global overturning circulation through the Indian, Pacific, and Southern Oceans: Schematics and transports. *Oceanography*, *26*(1), 80–97.

Tamsitt, V., Abernathey, R. P., Mazloff, M. R., Wang, J., & Talley, L. D. (2018). Transformation of deep water masses along Lagrangian upwelling pathways in the Southern Ocean. *Journal of Geophysical Research: Oceans*, *123*, 1994–2017. https://doi.org/10.1002/2017JC013409

Thomas, J. L., Waugh, D. W., & Gnanadesikan, A. (2015). Southern Hemisphere extratropical circulation: Recent trends and natural variability. *Geophysical Research Letters*, *42*, 5508–5515. https://doi.org/10.1002/2015GL064521

Walin, G. (1982). On the relation between sea-surface heat flow and thermal circulation in the ocean. *Tellus*, *34*, 187–195.

Worthington, L. V. (1981). The water masses of the world ocean: Some results of a fine-scale census. In B. A. Warren & C. Wunsch (Eds.), *Scientific surveys in honor of Henry Stommel* (pp. 42–69). Cambridge, MA: MIT Press.

Zika, J. D., England, M. H., & Sijp, W. P. (2012). The ocean circulation in thermohaline coordinates. *Journal of Physical Oceanography*, *2*, 708–724. https://doi.org/10.1175/JPO-D-11-0139.1

Zika, J. D., Sloyan, B. M., & McDougall, T. J. (2009). Diagnosing the Southern Ocean overturning from tracer fields. *Journal of Physical Oceanography*, *39*, 2926–2940.

View publication stats